Mechanism of Drying Thick Porous Bodies During the Falling-Rate Period:

III. Analytical Treatment of Macroporous Systems

A. H. NISSAN, H. H. GEORGE, JR., and T. V. BOLLES

Rensselaer Polytechnic Institute, Troy, New York

The analysis of a drying process requires a knowledge of the temperature of the material as a function of time and position. Previous work (*1*, *2*) has shown the existence of a unique temperature obtained during the falling-rate period—the *pseudo-wet-bulb temperature*.

Figure 1 represents a generalized time-temperature plot for a porous body being dried in air. The curve $A' B' C'$ represents the rate of drying; the other curves give the temperature distribution. The portion $A' B'$ of the rate-of-drying curve is the constant-rate period during which the temperature of the bed tends toward the wet-bulb temperature of the air. When the critical moisture content is reached, that is point B', the drying rate decreases and the liquid surface recedes below the surface of the bed. During the falling-rate period the temperature of the wet portion of the bed tends toward the pseudo-wet-bulb temperature. The curve DD' portrays the temperature of the surface of the bed. Since the surface of the bed is dry at all times during the falling-rate period, its temperature immediately tends to equal the temperature of the air.

The curves DEE' and DFF' represent the temperature histories of internal points in the bed, showing how they first reach the pseudo-wet-bulb temperature and later, as the points pass into the dry portion, reach the air temperature. DGG' is the curve representing the temperature history of the bottom of the bed. When point G is reached, the bed is dry and all the temperature curves rise more sharply toward the air temperature, because the heat entering the bed is manifest entirely as sensible heat, whereas before dryness part of the heat went to supply the latent heat of vaporization.

In part I (*1*) an implicit equation was presented for determining the pseudo-wet-bulb temperature:

$$k_e (t_a - t_{pwb}) = 2.88 \times 10^{-4} (\epsilon D)_{pwb} \lambda_{pwb} \left(\frac{P_{pwb}}{T_{pwb}} - \frac{p_a}{T_a} \right) \qquad (1)$$

in consistent c.g.s. units when water was the drying liquid.

In part II (*2*) it was shown that S, the pore liquid content or the degree to which pores are saturated with liquid in the wet portion, is not constant during the falling-rate period but decreases with time.

The intent of this paper is to show the generality of the pseudo-wet-bulb temperature, to present an explicit method of calculating the pseudo-wet-bulb temperature and the manner in which the bed rises to this new temperature, and finally to present equations suitable for predicting the rate of drying and the drying curves. These analyses apply, strictly, only to systems with relatively large pores—textiles or particulate systems like sand—since the exact behavior of gels and other collodial systems has not as yet been determined.

APPARATUS

The loop dryer was constructed of 8-by 12-in. by 21-gauge steel duct and was covered with 1 in. of asbestos insulation. The sample pan was 6 by 2 in. long dimension in the air direction, and 1-¼ in. deep. The pan was made from ¼-in. plywood and lined with polyethylene and epoxy resins to make it waterproof. Throughout the pan were located ten thermocouples at various depths.

The material that was dried was silica sand of − 16 + 20 mesh. The effective

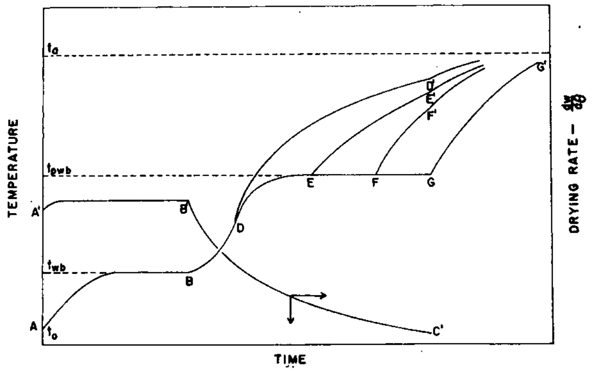

Fig. 1. Generalized time-temperature record.

thermal conductivity of the sand was determined to be 0.1645 Btu/(hr.)ft² (°F./ft.), and the void fraction was found to be 0.45.

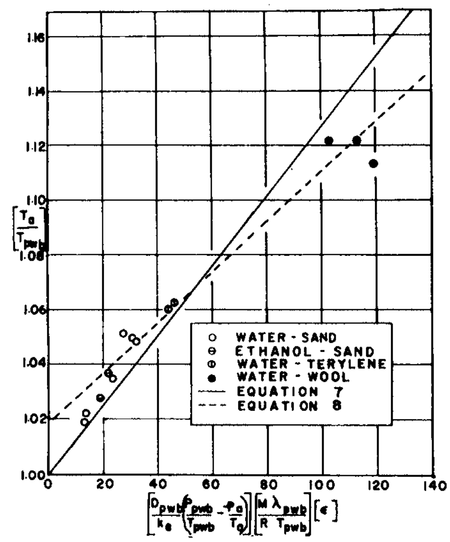

Fig. 2. Pseudo-wet-bulb temperature as a function of dimensionless groups.

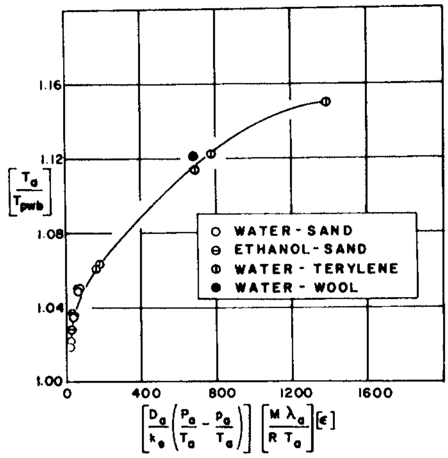

Fig. 3. Pseudo-wet-bulb temperature as a function of air temperature.

CALCULATION OF PSEUDO-WET-BULB TEMPERATURE

The drying of a wet material will be considered to have proceeded well into the falling-rate period and the evaporation to be taking place from a liquid surface well within the material. The liquid surface is a distance x from the surface of the bed, and the differential layer of bed just above the liquid surface through which must pass the entire heat required to vaporize the liquid will be considered. Hence

$$q = -k_e A_H \frac{dt}{dx} = -\frac{dW}{d\theta}\lambda_{pwb} \quad (2)$$

The rate of evaporation is assumed to be controlled by vapor diffusion. Then

$$-\frac{dW}{d\theta} = (\epsilon D)_{pwb} A_M \frac{dC}{dx} \quad (3)$$

$(\epsilon D)_{pwb}$ is the vapor diffusion coefficient at the temperature of the liquid surface corrected for the presence of the solid (assumed to have zero diffusion) by the void fraction ϵ.

The shapes of temperature and concentration curves are usually similar, and so it can be assumed that

$$\frac{\dfrac{dt}{dx}}{\dfrac{t_a - t_{pwb}}{x}} = \frac{\dfrac{dC}{dx}}{\dfrac{C_a - C_{pwb}}{x}} \quad (4)$$

and from the ideal gas law

$$C = \frac{M_L P}{RT} \quad (5)$$

Substituting Equations (3), (4), and (5) into Equation (2) yields

$$k_e(t_a - t_{pwb}) = 1.285 \times 10^{-3} (\epsilon D)_{pwb}\lambda_{pwb}\frac{M_L}{R}\left[\frac{P_{pwb}}{T_{pwb}} - \frac{p_a}{T_a}\right] \quad (6)$$

where R = 1.98 B.t.u./(lb.-mole)(°F.). Equation (6) can be rearranged to read

$$\frac{T_a}{T_{pwb}} = 1 + 1.285 \times 10^{-3} \left[\frac{D_{pwb}}{k_e}\left\{\frac{P_{pwb}}{T_{pwb}} - \frac{p_a}{T_a}\right\}\right]\left[\frac{M_L\lambda_{pwb}}{RT_{pwb}}\right][\epsilon] \quad (7)$$

The pseudo-wet-bulb temperature was calculated by means of Equation (6) for runs in which wool, terylene (British form of a polyester fiber), and sand were dried. In addition to drying water from all the materials, the ethanol-sand system was used for some runs.

The results were then plotted in the manner suggested by Equation (7) in Figure 2. A straight line was fitted through the points. The line of the form of Equation (7) is

$$\frac{T_a}{T_{pwb}} = 1.0185 + 1.111 \times 10^{-3} \left[\frac{D_{pwb}}{k_e}\left\{\frac{P_{pwb}}{T_{pwb}} - \frac{p_a}{T_a}\right\}\right]\left[\frac{M_L\lambda_{pwb}}{RT_{pwb}}\right][\epsilon] \quad (8)$$

Equation (7) is also shown in Figure 2.

The solution of Equation (8) for T_{pwb} still involves a trial-and-error procedure, since T_{pwb} appears on both sides of the equation. Since Equation (8) is dimensionally correct, the ratio T_a/T_{pwb} was calculated evaluating the properties of the liquid at the air temperature. These results are shown in Figure 3, which may be used to give T_{pwb} for the system directly from a knowledge of the air temperature and humidity. Thus the need for a trial-and-error method of calculating T_{pwb} is eliminated.

THE APPROACH TO PSUEDO-WET-BULB TEMPERATURE

With the pseudo-wet-bulb temperature rendered predictable, it is next

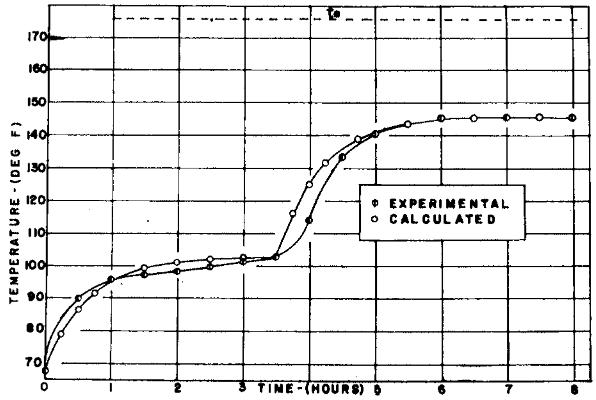

Fig. 4. Temperature of wet sand vs. time.

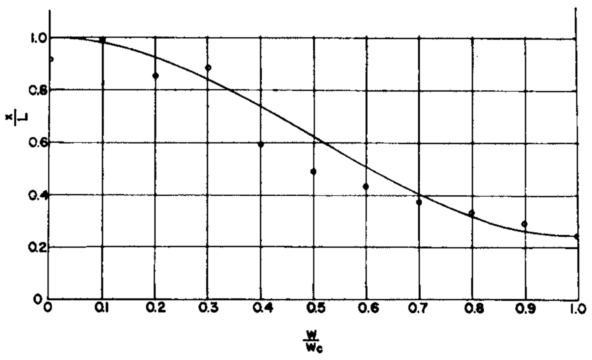

Fig. 5. Liquid distribution function.

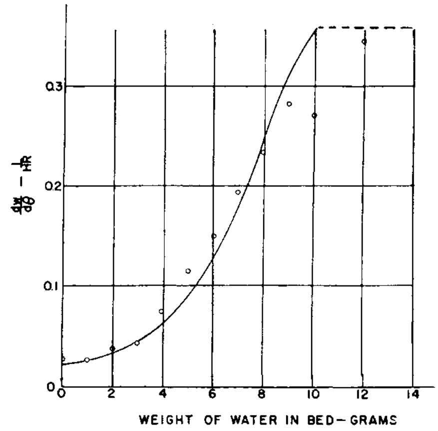

Fig. 6. Rate of drying curve.

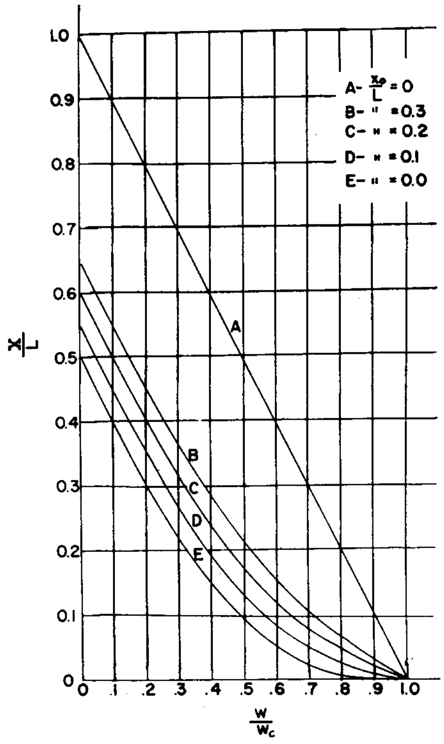

Fig. 7. Working plot 1.

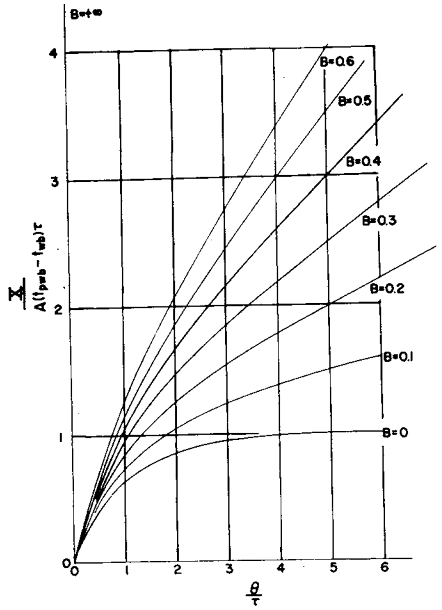

Fig. 8. Working plot 2.

necessary to describe the manner in which the bed approaches the pseudo-wet-bulb temperature once the critical moisture content is reached, that is point B' on Figure 1. Figure 1 suggests a first-order response to a step function of a resistance-capacitance complex. In other words the bed is behaving as if it were suddenly immersed, when it is at t_{wb}, into a bath at t_{pwb}. To simplify the analysis a flat bed will be assumed; for cylindrical or spherical bodies more complicated geometrical factors enter.

The wet portion of the bed is assume to be immersed in a virtual bath at the pseudo-wet-bulb temperature. (The excess temperature $t_a - t_{pwb}$ goes toward evaporating the liquid.) Then the sensible heat of the bed is given by

$$q = \frac{A_H}{R_H}(t_{pwb}-t) = V\bar{\rho}\,\bar{c}_P\frac{dt}{d\theta} \qquad (9)$$

and the boundary condition at

$$t = t_{wb} \text{ at } \theta = 0 \qquad (9a)$$

The solution to (9 and 9*a*) is known to be (3)

$$\frac{t-t_{pwb}}{t_{wb}-t_{pwb}} = e^{-\theta/(L-x_o)\overline{\rho c_P}R_H} \qquad (10)$$

$\theta = 0$ at critical moisture content
One defines

$$R_H = \frac{(L-x_o)}{\bar{k}} \qquad (11)$$

and then

$$\tau = \frac{L^2\bar{\rho}\bar{c}_P}{\bar{k}} =$$

$$\frac{L^{(L-x_o)^2}[(1-\epsilon)\rho_s c_{Ps}+\epsilon S_c\rho_L c_{PL}]}{k_e+\epsilon S_c k_L} \qquad (12)$$

or in terms of the critical moisture content Equation (12) may be expressed as

$$\tau = \frac{(L-x_o)^2\left[\rho_s c_{Ps}(1-\epsilon) + w_c\left(\frac{L}{L-x_o}\right)\rho_B c_{PL}\right]}{k_e + w_c\left(\frac{L}{L-x_o}\right)\frac{\rho_B}{\rho_L}k_L} \qquad (12a)$$

Hence

$$t = t_{wb} + (t_{pwb}-t_{wb})(1-e^{-\theta/\tau}) \qquad (13)$$

Equation (13) is compared with an experimental run in Figure 4.

TABLE 1

Run	Experimental W_c	Calculated w_c	System
4	0.040	0.023	Sand, water
5	0.034	0.028	Sand, water
6	0.052	0.036	Sand, water
12	0.030	0.026	Sand, water
13	0.033	0.033	Sand, water

The temperature driving force for conduction through the dry portion of the bed is then given by

$$(t_a - t) = (t_a - t_{pwb}) + (t_{pwb} - t_{wb})e^{-\theta/\tau} \qquad (14)$$

It is interesting to note that the rise from initial temperature to wet-bulb temperature at the beginning is given by the same τ value by the equation

$$t = t_o + (t_{wb} - t_o)(1-e^{-\theta/\tau}) \qquad (15)$$

LIQUID DISTRIBUTION

In order to derive a rate of drying equation, it is further necessary to know the location of the liquid surface as a function of time. Again only flat beds will be analyzed:

$$-k_e A_H\left(\frac{dt}{dx}\right) = -\lambda A_m L\rho_B\left(\frac{dw}{d\theta}\right) \qquad (16)$$

Assuming a linear temperature gradient through the dry portion of the bed, one can use $(\Delta t/\Delta x)$ for (dt/dx) and $\Delta x = -x$. Thus

$$x = \frac{-k_e}{\lambda L\rho_B}\,\frac{(t_a-t_{pwb})+(t_{pwb}-t_{wb})e^{-\theta/\tau}}{\frac{dw}{d\theta}} \qquad (17)$$

As the liquid evaporates, two events take place: the surface of the liquid recedes into the bed, and the thickness of the liquid film covering the pore walls decreases. Thus very complex hydrodynamic and thermal forces come into play, resulting in complicated flows. An approximate but empirical solution was attained as follows. Experimental values of θ and $dw/d\theta$ were substituted into Equation (17) in order to determine the nature of $w = \phi(x)$ function. The results suggested, for a flat bed, a cosine relationship:

$$\cos\left(\frac{w}{w_c}\pi\right) = 2\left(\frac{x-x_o}{L-x_o}\right) - 1 \qquad (18)$$

Equation (18) and some experimental points are presented in Figure 5. x_o in Equation (18) is obtained from Equation (17) by setting $\theta = 0$.

THE DRYING-RATE CURVE

Since $\Delta t = \Psi(\theta)$ and $x = \phi(w)$ are known, it is possible to write the drying rate equation. It is assumed that all

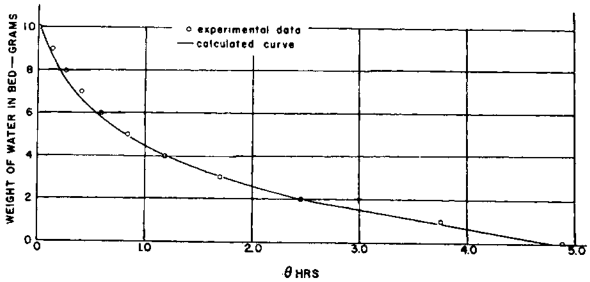

Fig. 9. Moisture-content vs. time curve.

faces except those for the drying surface of the bed are adiabatic, the area for heat transfer in the dry portion of the bed is equal to the area for mass transfer, and $(dt)/(dx) \cong (\Delta t)/(\Delta x)$ in the dry portion of the bed. In view of these assumptions Equation (16) may be written as

$$k_e \frac{\Delta t}{\Delta x} = \lambda L \rho_B \frac{dw}{d\theta} \qquad (16a)$$

Substituting Equations (14) and (18) into Equation (16*a*), one obtains

$$\frac{-k_e}{\lambda L \rho_B}\left[(t_a - t_{pwb}) + (t_{pwb} - t_{wb}) e^{-\theta/\tau} \right] d\theta = \left[\frac{L+x_o}{2} + \frac{L-x_o}{2} \cos\left(\frac{w}{w_c}\pi\right) \right] dw \qquad (19)$$

Equation (19) rearranges to give the drying rate explicitly:

$$\frac{dw}{d\theta} = \frac{-2k_e}{\lambda L \rho_B} \frac{(t_a - t_{pwb}) + (t_{pwb} - t_{wb}) e^{-\theta/\tau}}{(L+x_o) + (L-x_o)\cos\left(\frac{w}{w_e}\pi\right)} \qquad (20)$$

Figure 6 shows a comparison of Equation (20) with some experimental data.

On the basis that $dw/d\theta$ at time zero for the falling-rate period equals that for the constant-rate period, which can be independently evaluated, x_o can be calculated from Equation (17) by setting $\theta = 0$. Thus

$$x_o = \frac{-k_e (t_a - t_{wb})}{\lambda_{wb} L \rho_B \left(\frac{dw}{d\theta}\right)_{C.R.}} \qquad (21)$$

THE MOISTURE-CONTENT VS. TIME CURVE

The drying curve which gives the moisture content at different times is obtained by integration of Equation (20) with the limits of 0 to θ on $d\theta$ and w_c to w on dw. The resulting equation is

$$\frac{k_e}{\lambda L \rho_B W_c}\left[(t_a - t_{pwb})\theta + \tau(1 - e^{-\theta/\tau})(t_{pwb} - t_{wb}) \right] = \left\{ \left[\left(\frac{L+x_o}{2}\right)\left(1 - \frac{w}{w_c}\right) \right] - \left[\frac{L-x_o}{2\pi} \sin\left(\frac{w}{w_c}\pi\right) \right] \right\} \qquad (22)$$

In order to ease the use of Equation (22) it has been reduced to a graphical solution:

$$A = k_e/(\lambda L \rho_B W_c) \qquad (23)$$

$$B = \frac{t_a - t_{pwb}}{t_{pwb} - t_{wb}} \qquad (24)$$

$$X = \left(\frac{L+x_o}{2}\right)\left(1 - \frac{w}{w_c}\right) - \left(\frac{L-x_o}{2\pi}\right)\left(\sin\frac{w}{w_c}\pi\right) \qquad (25)$$

Substituting Equations (23), (24), and (25) into Equation (22) and rearranging, one gets

$$\frac{X}{A\tau(t_{pwb} - t_{wb})} = B\frac{\theta}{\tau} + (1 - e^{-\theta/\tau}) \qquad (26)$$

and

$$\frac{X}{L} = \left(\frac{1 + \frac{x_o}{L}}{2}\right)\left(1 - \frac{w}{w_c}\right) - \left(\frac{1 - \frac{X_o}{L}}{2\pi}\right)\left(\sin\frac{w}{w_c}\pi\right) \qquad (27)$$

Equation (27) is plotted in Figure 7 as a family of curves, X/L vs. w/w_c with x_o/L as the parameter. Equation (26) is plotted in Figure 8 as a family of curves θ/τ vs. $X/[A\tau(t_{pwb} - t_{wb})]$ with B as the parameter. To use Figures 7 and 8, one enters Figure 7 at a predetermined value of x_o/L and w/w_c and reads X/L. X/L is then multiplied by the group $L/[A\tau(t_{pwb} - t_{wb})]$ and entered into Figure 8 at the proper value of B; a value of θ/τ is obtained. τ is defined by Equation (12). Thus with a knowledge of t_a, t_{wb}, t_{pwb}, w_c, $(dw/d\theta)_{C.R.}$ and the thermal properties of bed and fluid, it is possible to calculate the drying curve. Figure 9 compares Equation (22) with experimental data.

DISCUSSION

The equations developed appear to define the drying process fairly well in spite of one arbitrary function imposed on the equations. This simplifying arbitrary function was imposed because a complete *a priori* derivation would demand the formulation of the laws of the fluid dynamics of nonisothermal flow through porous media. The present analysis was limited to heat and mass transfer considerations in the interests of simplicity. Hence a cosine function was adopted to describe the flow of the liquid inside the bed.

w_c is generally defined as the moisture content obtained by extrapolating the constant-rate curve and the falling-rate curve (*4, 5*). The calculated values of w_c were obtained by choosing the best values of w_c in Equation (22) which gave agreement between the calculated and the experimental time to dryness. The calculated and experimental values of w_c for some runs are shown in Table 1.

SUMMARY

The pseudo-wet-bulb temperature is found to exist in particulate as well as in fibrous materials. The equations for predicting the pseudo-wet-bulb temperature are the same, and its calculation is rendered explicit by the presentation of a chart.

An equation for the drying rate as a function of time is derived:

$$\frac{dw}{d\theta} = \frac{-2k_e}{\lambda L \rho_B} \frac{(t_a - t_{pwb}) + (t_{pwb} - t_{wb}) e^{-\theta/\tau}}{(L+X_o) + (L-X_o)\cos\left(\frac{w}{w_c}\pi\right)}$$

This is integrated to give the equation for the moisture content as a function of time:

$$\frac{k_e}{\lambda L \rho_B W_c}\left[(t_a - t_{pwb})\theta + \tau(1 - e^{-\theta/\tau})(t_{pwb} - t_{wb}) \right] = \left\{ \left[\left(\frac{L+x_o}{2}\right)\left(1 - \frac{w}{w_c}\right) \right]\right.$$

$$-\left[\left(\frac{L-x_o}{2\pi}\right)\sin\left(\frac{w}{w_c}\pi\right)\right]\Bigg\}$$

Finally, to facilitate the use of this equation it is reduced to a graphical solution.

NOTATION

A = parameter defined by Equation (23)
A_H = heat transfer area, sq. ft.
A_M = mass transfer area, sq. ft.
B = parameter defined by Equation (24)
C = vapor concentration, lb./cu. ft.
C_P = specific heat at constant pressure, B.t.u./(lb.)(°F.)
D = volumetric diffusivity, sq. ft./hr.
k_e = effective thermal conductivity of solid, B.t.u./(hr.)(ft.)(°F.)
k_L = thermal conductivity of liquid, B.t.u./(hr.)(ft.)(°F.)
L = total depth of bed, ft.
M_L = molecular weight of liquid
P = vapor pressure, lb./sq. in.
p = partial pressure, lb./sq. in.
R = universal gas constant, B.t.u./lb. mole °F.
R_H = resistance to heat transfer, sq. ft. hr. °F./B.t.u.
S = pore liquid content or saturation, cu. ft. liquid/cu. ft. of void space in wet portion of bed
T = absolute temperature, °R.
t = temperature, °F.
V = bed volume, cu. ft.
W = total weight of bed, lb.
w = free moisture content, lb. liquid/lb. bed
x = depth of liquid surface from bed surface, ft.
X = parameter defined by Equation (25)

Greek Letters

ϵ = void fraction, volume voids/volume bed
λ = latent heat of vaporization, B.t.u./lb.
ρ_B = density of dry bed, lb./cu. ft.
ρ_L = density of liquid, lb./cu. ft.
τ = time constant for the system, hr.

Subscripts

o = property evaluated at initial bed temperature
wb = property evaluated at wet-bulb temperature of the air
pwb = property evaluated at pseudo-wet-bulb temperature
a = property evaluated at air temperature
c = indicates the property value at critical moisture content
$C.R.$ = property evaluated at the constant rate of drying condition

Superscripts

$-$ = average property for entire bed

LITERATURE CITED

1. Nissan, A. H., W. G. Kaye, and J. R. Bell, *A.I.Ch.E. Journal*, **5**, 103 (1959).
2. Bell, J. R., and Nissan, A. H., *ibid.*, **5**, 344 (1959).
3. Schneider, P. J., "Conduction Heat Transfer," Addison-Wesley, Reading, Mass. (1955).
4. McCabe, W. L., and J. C. Smith, "Unit Operations," McGraw-Hill, New York (1956).
5. Badger, W. L., and J. T. Banchero, "Introduction to Chemical Engineering," McGraw Hill, New York (1955).

Manuscript received August 18, 1959; revision received October 30, 1959; paper accepted November 17, 1959.

Mass Transfer in Laminar—Boundary-Layer Flows with Finite Interfacial Velocities

ANDREAS ACRIVOS

University of California, Berkeley, California

Asymptotic expressions are presented in this paper for the mass transfer Nusselt number in both forced- and free-convection laminar-boundary-layer flows with large interfacial velocities directed toward the surface. The analysis is valid for arbitrary surface geometries and includes transfer in a variable properties fluid. It is shown, in addition, how these asymptotic formulas may be used in conjunction with the Nusselt number for zero interfacial velocities to estimate the rate of mass transfer for the intermediate regions.

In mass transfer operations the surface past which the fluid moves has the additional property of acting as a source or a sink of material to the flowing stream. Strictly speaking, therefore, mass and heat transfer are not completely analogous phenomena, even under seemingly identical flow configurations; in the formal case the interfacial velocity is usually finite, rather than identically zero, owing to the material exchange on the surface. In particular, the breakdown of the analogy between mass and heat transfer is most pronounced when the mole fraction of the diffusing species is almost zero near the surface and almost unity in the main stream (or vice versa), for then the normal component of the hydrodynamic velocity at the surface is